

Experimental Validation of Moving Spring-Mass-Damper Model for Human-Structure Interaction in the Presence of Vertical Vibration

Ehsan Ahmadi¹, Colin Caprani^{2*}, Stana Živanović³, Amin Heidarpour¹

¹ School of Engineering and the Built Environment, Birmingham City University, UK

² Dept. of Civil Engineering, Monash University, Australia

³ School of Engineering, University of Exeter, UK

* Corresponding Author

Abstract

The interaction between structures and walking humans is an important factor in vibration serviceability assessment of slender, lightweight, and low-damping structures. When on bridges humans form a human-structure system and interact with the structural vibration. The conventional vertical moving force (MF) model neglects human-structure interaction (HSI) effects. In contrast, a moving spring-mass-damper (MSMD) model is shown to have the potential to incorporate HSI effects leading to more accurate vibration response prediction. The MSMD model parameters have been much studied in biomechanics. However, the literature lacks an experimental calibration of the MSMD model parameters on a vibrating surface for vibration serviceability design and assessment purposes. Consequently, an experimental-numerical methodology is developed to calibrate the MSMD model parameters in the worst-case (resonance) scenario by matching measured and simulated vibration responses. To facilitate simple implementation of HSI effects into engineering practice, results of simulation using a calibrated equivalent moving force (EMF) model are also shown. The walking force on rigid surfaces along with vibration responses of two lively full-scale laboratory footbridges are measured for 23 test subjects by performing a total of 295 trials on the two structures. A parametric study is first performed on the MSMD model using the experimental results. The experimental results of the Monash footbridge are then used as the training dataset to extract optimal MSMD model parameters. The results from the Warwick footbridge are used to

validate the model. The validation tests results show a considerable improvement in the vibration response prediction using both models. It was found that when walking in resonance with the bridge, the walker can be modelled to have natural frequency equal to the resonant frequency of the bridge, and that the damping ratio is larger for heavier walkers.

Keywords human-induced vibration, human-structure interaction, moving spring-mass-damper model, equivalent moving force model, vertical walking force.

1. Introduction

1.1 Background

Many modern structures are vibrationally-vulnerable to human activities, especially with the growing use of high-strength and lightweight materials in the construction industry. Human activities such as walking, jumping, and running may induce uncomfortable vibrations and result in structural serviceability failure and associated economic and social losses. Hence, accurate assessment of structural vibration is an essential step in ensuring that the design of structures is fit for their intended purpose.

To estimate pedestrian-induced vibrations of structures, knowledge of not only structure dynamics, but also dynamics of the human body, might be required. Different approaches exist in modelling pedestrian effects on the structure. A basic model simulates human walking as a moving force (MF) that crosses the structure at a constant velocity. This force in the time domain is of a well-known M-shape, but it is often represented as a single harmonic that can excite the resonance of the structure (which is deemed to be most relevant) [1]. The MF model often overestimates structural vibration response as it ignores interaction between the human body dynamics and dynamics of the supporting structure ([2],[3],[4]). An improvement on the

MF model, that is increasingly used in recent human-induced vibration studies [5], is to represent the pedestrian as a moving spring-mass-damper (MSMD) model ([3], [6]). However, there remains a challenge to calibrate the MSMD model parameters using experimental data before the model can be recommended for use in the design guidelines.

1.2 Models for pedestrians

Many guidelines have used a MF model to evaluate vibration serviceability of footbridges (e.g., OHBDC [7], BS 5400 [8], ISO-10137 [9], Eurocode 5 [10], Setra [11], HIVOSS [12]). The model is developed based on experimental data for ground reaction forces collected using force plate and/or instrumented treadmill mounted on stiff laboratory floors; i.e., it represents the dynamic force imparted by the pedestrian on a rigid surface. Consequently, the influences of mass, damping, and stiffness of the human body, along with any walking force alteration due to the vibration of the supporting surface, are neglected. This approach was found to be mostly acceptable for older generation structures that were heavier and less slender than their modern counterparts. As a result, the MF model has been embedded not only in the vibration serviceability design guidelines but also into engineering practice software, and it has become a regular feature in the vibration assessment. But for contemporary slender light structures, the appropriateness of the MF model is being increasingly questioned. Recognising the need for both improved accuracy of vibration prediction and preserving the simplicity of the calculation process, an equivalent MF model (EMF) has been proposed recently [13]. The EMF model returns a similar vibration response to the more elaborate SMD model by tuning the bridge damping, thereby implicitly accounting for HSI. However, the parameters of the SMD, and consequently those of EMF are not yet experimentally validated.

There exists increasingly convincing experimental evidence that pedestrians' presence on the bridges alters the dynamics of the supporting deck by altering both its damping and natural frequency ([2],[14], [15], [16], [17]). It is also becoming accepted that one of the main harmonics of walking force gets attenuated when its frequency is close or equal to the frequency of structural vibration ([18], [19], [20], [21]). Representing a pedestrian on a vibrating bridge as a linear MSMD model makes it possible to decompose the imparted walking force into two components: (1) a notional walking force (as imparted on a rigid surface) and (2) the interaction force caused by vibration of the deck [3]. This approach is beneficial because it utilises the rigid-surface walking force (MF) model that is well developed over several decades ([9], [22],[23],[24]). What remains to be done is to calibrate and validate the interaction force part of the model, that relies on identification of mass, spring, and damping coefficients of the human body in a walking posture. It is because of this lack of knowledge that MSMD models are not yet common in engineering practice, even though they are regularly used in research.

To use the MSMD model, accurate parameters are clearly essential to obtain good predictions of vibration response. These parameters have been much-investigated in biomechanical engineering applications using measurements of rigid surface walking forces and accelerations of the human body centre of mass ([25],[26],[27],[28],[29],[30],[31]). For structural vibration, Archbold [32], Caprani et al. [33], Archbold et al. [34], and Ahmadi et al. [13] adopted the MSMD model parameters from the biomechanics literature. Hashim et al. [35] determined dynamic properties of the standing (stationary) human body. Xiaong et al. [36] proposed an SMD model for human-structure interaction during crowd jumping, and calibrated the model using the bridge laboratory at Monash University. Silva and Pimentel's work [37] proposed ranges for the MSMD model parameters using a synthetic walking force model rather than

measured walking forces. Toso et al. [38] used the measured vertical walking force on a rigid surface as well as the acceleration at the waist level of the test subjects and determined the MSMD model parameters using the acceleration frequency response function of the test subjects. They verified the model on a full-scale footbridge. However, this bridge is quite stiff giving maximum acceleration up to just 0.4 m/s^2 (small levels of human-structure interaction) and so the identified parameters may not be suitable for more flexible footbridges where higher levels of acceleration are expected. Shahabpoor et al. [39] proposed statistical distributions for the MSMD model using modal tests based on frequency response functions, but no validation of the parameters was presented for vibration response prediction. Recently, Zhang et al. [40] proposed a biomechanically-excited MSMD model for consideration of HSI in which the internal muscle force was represented via an internal actuator acting on both human and structure. This model accounts for biomechanical forces and suggests a constant damping ratio of 0.3. The model damped frequency is assumed to be equal to the pacing frequency [41]. Therefore, their model assumed the human body is experiencing resonance whilst walking and has a constant damping ratio of 0.3. A single damping ratio for all pedestrians is not a valid assumption as people clearly have different body characteristics and consequently different damping ratios. The internal biomechanical (or actuator) force was also determined from measurements on a stiff floor. Overall, there is not yet experimental calibration and validation of the MSMD model parameters on lively footbridges for a range of test subjects and trials.

1.3 Contribution

The preceding literature survey shows that there is a need to calibrate and validate the MSMD model using experimental data taken from lively structures. To address this need, an experimental-numerical framework using the vertical acceleration response of two lively footbridges is developed. Ground reaction forces generated by people walking on rigid surface

are measured. The experimental results of one footbridge are used to calibrate MSMD model parameters by matching measured and simulated vibration responses. The adequacy of the proposed MSMD and performance of EMF model parameters are tested against the experimental results of the second footbridge. The results show a good agreement between the responses of the proposed models and the measured footbridge responses. As such, the MSMD parameters should find good use in further research, and perhaps future engineering practice software, while the EMF parameters can find immediate application in practice.

2. Experimental Tests

2.1 Full-scale footbridges

The two full-scale laboratory footbridges used are: (1) the Monash Bridge (MB), shown in Figure 1a, which is constructed from epoxy-bonded pultruded glass fibre reinforced polymer (GFRP) located in Monash University, Australia, and (2) the Warwick Bridge (WB), shown in Figure 1b, a steel-concrete composite footbridge located in the University of Warwick, UK. The first natural frequency, f_b , damping ratio, ζ_b , and modal mass, M_b , of the first vertical flexural vibration mode along with span length, L_b , of both footbridges are summarized in Table 1.

The MB is a lightweight structure with a natural frequency within the range of the third harmonic of walking force, about 5.6 Hz. In contrast, the WB is a comparatively much heavier structure with first natural frequency just within the range of the first harmonic of walking force, about 2.4 Hz. The different properties of these two footbridges provide an opportunity for more elaborate evaluation of the MSMD modelling approach.

Table 1. Relevant properties of the Monash and Warwick footbridges (see text for symbols).

Footbridge	f_b (Hz)	ζ_b (%)	M_b (kg)	m_b (kg/m)	L_b (m)
------------	------------	---------------	------------	--------------	-----------

Monash Bridge (MB)	5.6	0.6	487	92.5	8.7
Warwick Bridge (WB)	2.4	0.3	7614	829.0	16.2

(a)



(b)



Figure 1. Two full-scale laboratory footbridges: (a) MB, 5.6 Hz (b) WB, 2.4 Hz.

2.2 Walking trials

Extensive walking experiments were conducted on both Monash and Warwick footbridges. These experiments are described in detail in two companion papers [42], [43]. Only a summary

of the necessary aspects of the trials are reported here. The interested reader should refer to the other papers for further details.

For each walking trial, a test subject walked a circuit of a bridge surface (BS) and a rigid surface (RS), Figure 2. The walking length, L_w , was the same for both surfaces (see Figure 2 – 13.0 m and 16.2 m, respectively for the Monash and Warwick footbridges). A metronome was used in trials in which the test subject was required to target a particular pacing (walking) frequency.

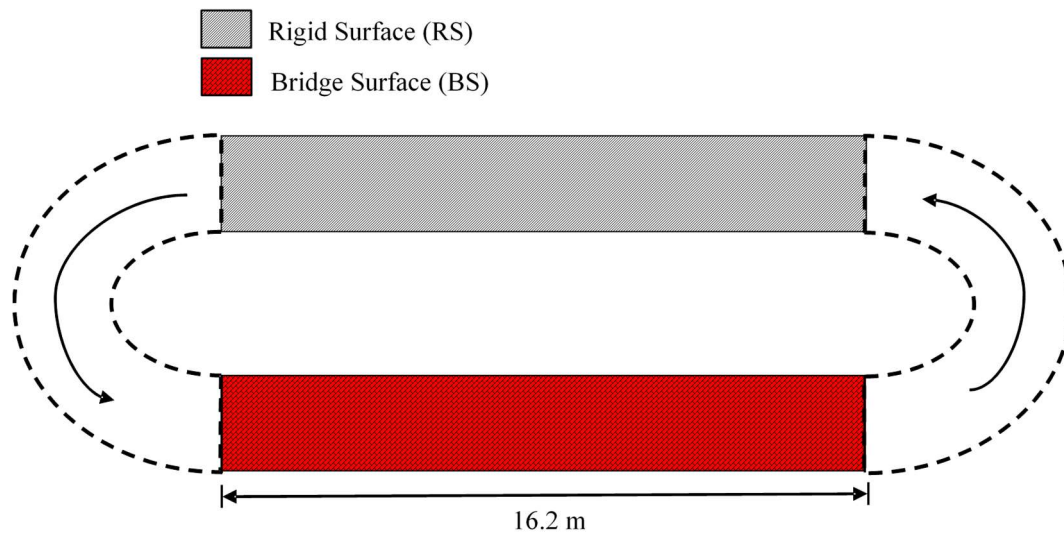


Figure 2. Schematic plan of a walking trial.

The MB trials comprised of walking at 1.86 Hz (third harmonic resonant walking). This walking frequency, f_w , was repeated to reach 15 successful walking trials for each test subject. For the WB, the trials consisted of 2.4 Hz (first harmonic resonant walking). Five acceptable trials were required at the walking frequency for each test subject. Eighteen test subjects (9 males and 9 females) participated in the tests on the MB, resulting in $18 \times 15 = 270$ recorded trials. The selected test subjects had no indications of any medical walking-related problems. The weight and gender of each test subject are specified in Table 2. For the WB, five test subjects (4 males and 1 female), took part in the testing (see Table 3) resulting in $5 \times 5 = 25$

recorded trials. Again, the selected test subjects had no indications of any medical walking-related problems.

Table 2. Test subjects of the MB experiments.

Test Subject No.	Weight (N)	Gender
1	865	M
2	718	M
3	654	M
4	444	F
5	678	M
6	862	M
7	717	M
8	970	M
9	522	F
10	1063	M
11	647	F
12	773	F
13	495	F
14	609	F
15	509	F
16	683	F
17	1489	F
18	1112	M

Table 3. Test subjects of the WB experiments.

Test Subject No.	Weight (N)	Gender
1	543	M
2	646	F
3	793	M
4	968	M
5	1117	M

The tests on the MB were more extensive. For this reason, the experiments on the MB are used for calibration of MSMD model. The WB trials are then used to validate the model. Previous studies on the Monash and Warwick footbridges ([43]and [42]) show that the effects of HSI were observed in both bridges through an alteration of the imparted walking forces and dynamic properties of the structure. These effects were most pronounced in the design-critical scenario of resonant walking. Therefore, the results of resonant walking experiments are used

in the MSMD model calibration process as it is both the critical design consideration and exhibits most HSI.

2.3 Experimental results

During each trial, the acceleration responses of the footbridge and the vertical walking force on the rigid surfaces were measured. Figure 3a shows the vibration response to excitation in resonance with the third harmonic of the dynamic force measured on the MB. Although the short span of the footbridge does not allow for a stationary resonant response, human-structure interaction effects still exist due to the high vibration of the footbridge at resonance. Figure 3b shows the resonance caused by walking at 2.4Hz on the WB. These two responses are for the only test subject who participated in the experiments on both bridges; specifically test subject no. 18 (and trial no. 7) on the MB and test subject no. 3 (and trial no. 3) on the WB. Note that this person and these two trials are used as illustrative examples throughout the paper. A 4th order zero-phase band-pass Butterworth filter was used to filter the vibration responses of each footbridge to isolate the dominant fundamental mode. The high vibration levels in Figure 3, up to about 2 m/s^2 , indicate the liveliness of both bridges under human walking.

In contrast to previous studies that used the instrumented treadmills to record multiple-step force whilst walking on the spot, in this study the force time histories were recorded during the actual traverses of the bridge decks. To achieve this, in-shoe sensors, specifically the Tekscan F-scan in-shoe foot pressure sensors, were used [44], [45]. These sensors provide plantar force-time histories for each foot. The left and right feet forces are then summed up to obtain the total vertical walking force. Figures 4a and 4b show the total force measured on the rigid surface for the exemplar test subject. The Tekscan sensors have many important aspects to consider so that

reliable measurements are obtained. Quality control measures were employed to ensure minimising measurement errors, as explained in more detail in [42] and [43].

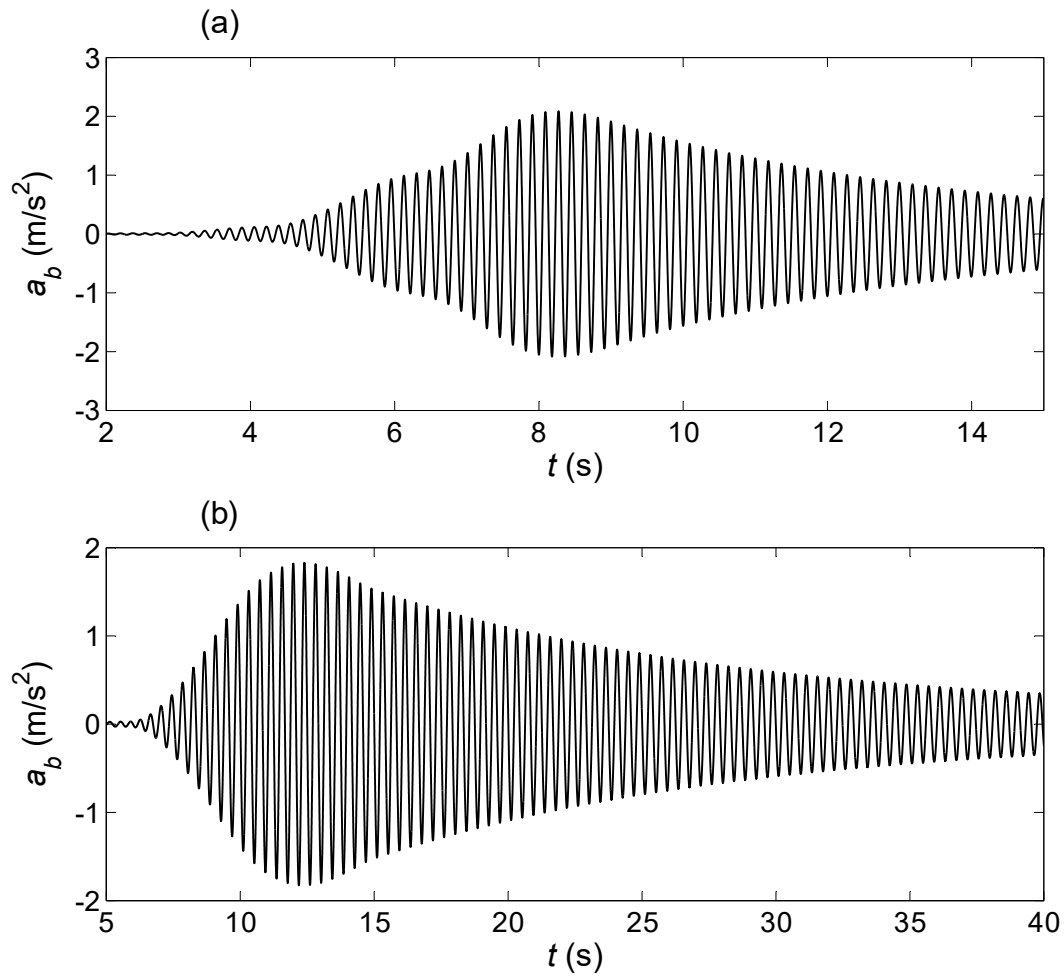


Figure 3. Mid-span resonant walking accelerations for the same person on: (a) MB (test subject no. 18, trial no. 7) (b) WB (test subject no. 3, trial no. 3).

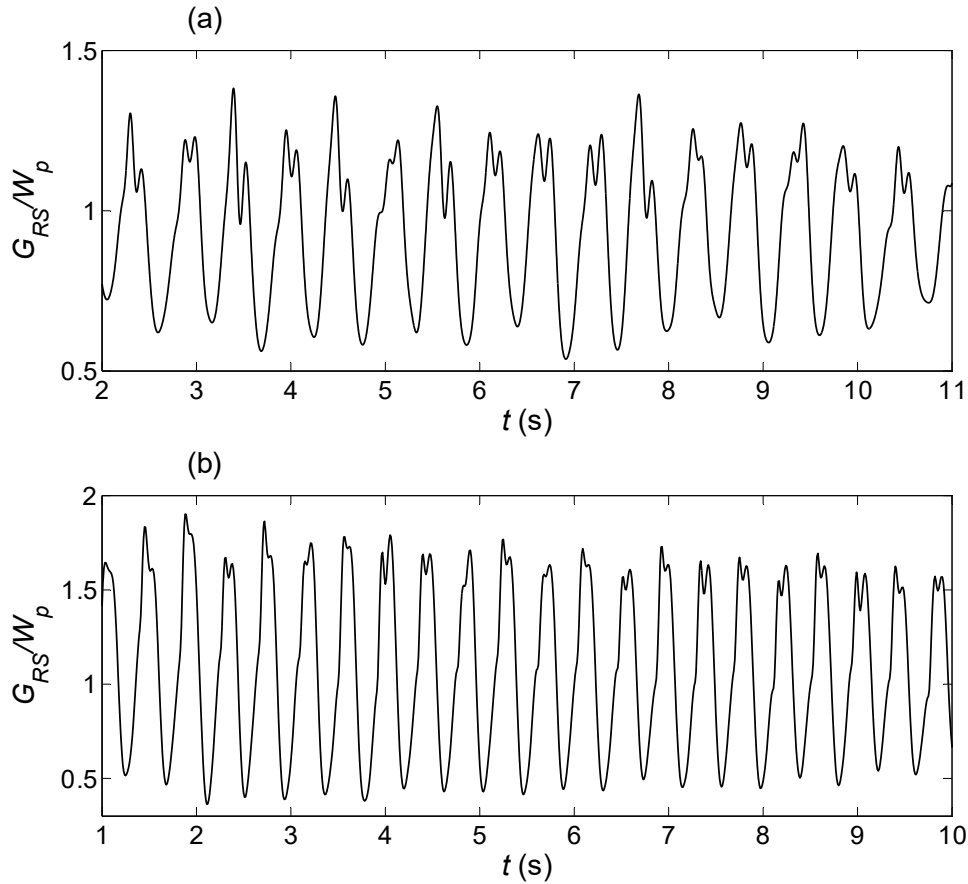


Figure 4. Force measured on the rigid surface with pacing rate that would excite resonance (if the walking was on the bridge) in the trials related to: (a) MB tests and (b) WB tests.

3. Pedestrian-Structure Models

In this section, the human-structure system models are formulated. Each footbridge is modelled as a simply-supported beam in modal space using its first vertical bending mode properties. This is adequate since both structures have well-spaced modes and the contribution of the first mode dominates the total response ([42], [43]). The walking pedestrian is modelled in three forms: MF, MSMD, and EMF.

3.1 MF-structure model

This model represents the pedestrian as a force generated on rigid surface— $G_{RS}(t)$ —and travelling at a constant velocity, v (Figure 5a). In this case, the modal force in the first mode is:

$$F_1(t) = \int_0^{L_b} G_{RS}(t) \delta(x - vt) \phi_1(x) dx \quad (1)$$

in which $\delta(\cdot)$ is the Dirac delta function required to locate the force on the footbridge and ϕ_1 is the arbitrarily-scaled footbridge mode shape, shown in Figure 5. Using the sifting property of the Dirac delta function, equation (1) becomes:

$$F_1(t) = G_{RS}(t) \phi_1(vt) \quad (2)$$

Therefore, the equation of motion in modal space is [5]:

$$\ddot{q}_1(t) + 2\xi_b \omega_b \dot{q}_1(t) + \omega_b^2 q_1(t) = \frac{\phi_1(x)}{M_b} G_{RS}(t) \quad (3)$$

where q_1 , \dot{q}_1 , and \ddot{q}_1 are the modal displacement, velocity, and acceleration for the first mode of the footbridge; ξ_b , ω_b , and M_b are the damping, circular natural frequency, and modal mass for the first mode of vibration. Finally, the acceleration response of the footbridge in physical coordinates at any location is:

$$\ddot{u}(x,t) = \phi_1(x) \ddot{q}_1(t) \quad (4)$$

3.2 MSMD-structure model

The pedestrian is modelled as a linear single-degree-of-freedom mechanical system (or MSMD) having mass, m_p , damping, $c_p = 2m_p\xi_p$, and stiffness, $k_p = m_p\omega_p^2$, where $\omega_p = 2\pi f_p$ (Figure 5b) crossing the structure at a contact speed v , whilst f_p and ξ_p are representing the natural frequency and damping ratio of the pedestrian's body, respectively. The equation of motion at the pedestrian's degree-of-freedom [5]:

$$m_p \ddot{y} + c_p (\dot{y} - \phi_1 \dot{q}_1) + k_p (y - \phi_1 q_1) = 0 \quad (5)$$

where y is the displacement of the mass from equilibrium position. The interaction force between the footbridge and MSMD model is [5]:

$$G_{BS}(x, t) = [G_{RS}(t) - m_p \ddot{y}] \delta(x - vt) \quad (6)$$

Equation (6) shows that a linear MSMD can be thought of as splitting the contact force on the bridge surface, G_{BS} , into the walking force on the rigid surface, G_{RS} , and the interaction force component, $-m_p \ddot{y}$. This reduction in the bridge surface force is supported by experimental evidence on both Monash and Warwick footbridges for resonant walking trials ([42], [43]).

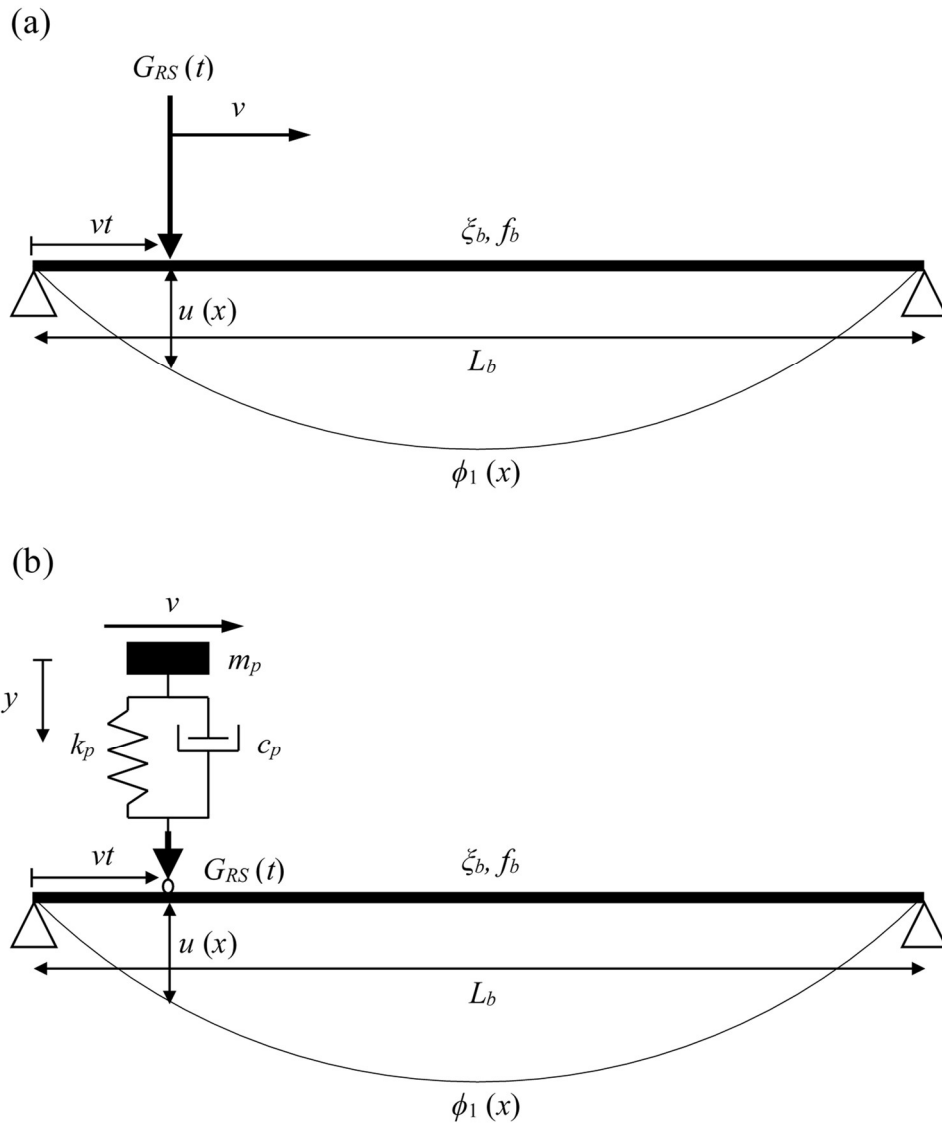


Figure 5. Human-structure models: (a) conventional moving force (b) interacting moving spring-mass-damper.

Equations (3) and (6) for the footbridge and (5) for the SMD can be expressed in two coupled equations as follows:

$$\begin{bmatrix} 1 & m_p \phi_1(vt) \\ 0 & m_p \end{bmatrix} \begin{Bmatrix} \ddot{q}_1 \\ \ddot{y} \end{Bmatrix} + \begin{bmatrix} 2\xi_b \omega_b & 0 \\ -c_p \phi_1(vt) & c_p \end{bmatrix} \begin{Bmatrix} \dot{q}_1 \\ \dot{y} \end{Bmatrix} + \begin{bmatrix} \omega_b^2 & 0 \\ -k_p \phi_1(vt) & k_p \end{bmatrix} \begin{Bmatrix} q_1 \\ y \end{Bmatrix} = \begin{Bmatrix} G_{RS}(t) \phi_1(vt) / M_b \\ 0 \end{Bmatrix} \quad (7)$$

This is solved using Newmark-Beta scheme to simulate vibration response of the bridge for a given set of SMD parameters. Before the main analysis, the time step of the analysis was reduced to the extent that any further reduction in the time step will not change the vibration response of the bridge.

3.3 EMF model

In this section, the previously-proposed equivalent moving force (EMF) system is briefly described [13]. In the time domain, a continuous walking force is commonly described using a Fourier series [46], [47], [48], [5]:

$$G(t) = W_p \sum_{k=0}^r DLF_k \cos(2\pi k f_w t + \varphi_k) \quad (8)$$

where $W_p = m_p g$ and m_p is the pedestrian mass, g is the acceleration due to gravity; f_w is the walking pacing frequency; and DLF_k is the dynamic load factor (DLF) for the k th harmonic. The phase angle of the k th harmonic is denoted by φ_k , and r represents total number of harmonics considered. In this representation, the harmonic $k = 0$ corresponds to the static pedestrian weight, and so $\varphi_0 = 0$ and $DLF_0 = 1$.

For the EMF system, the footbridge modal model is subjected to the k th harmonic of the walking force, $G_k^{RS} = DLF_k \cos(2\pi k f_w t + \varphi_k)$. Figure 6a shows the reference system, a stationary spring-mass-damper (SSMD) at the location of x_p (that is, “walking on the spot”) and Figure 6b shows an EMF system for the footbridge and resonant k th harmonic of the walking force. The steady-state vibration response of the reference SSMD system is matched by that of the EMF system through tuning the equivalent bridge damping ratio to [13]:

$$\zeta_b^{eq} = \frac{1}{2} \sqrt{\frac{\left(\frac{4\zeta_b\zeta_p}{\alpha} + \mu_1\phi_1^2\right)^2 + 4\left(\zeta_b\left(1 - \frac{1}{\alpha^2}\right) - \frac{1}{\alpha}\mu_1\phi_1^2\zeta_p\right)^2}{\left(1 - \frac{1}{\alpha^2}\right)^2 + 4\left(\frac{\zeta_p}{\alpha}\right)^2}} \quad (9)$$

where α is the SMD-to-bridge frequency ratio (i.e. $\alpha = f_p/f_b$) and μ_1 is the pedestrian-to- bridge modal mass ratio (i.e. $\mu_1 = m_p/M_b$). The response simulations in the EMF model then require using the equivalent damping ratio for the bridge to calculate the vibration responses of the bridge, which will be equivalent to the response that would be calculated in more demanding (from practitioner's point of view) MSMD simulations. When the frequency of the pedestrian is the same as the frequency of the bridge, then $\alpha = 1$ and equation (9) becomes:

$$\zeta_b^{eq} = \frac{\mu_1\phi_1^2}{2} \sqrt{1 + \left(\frac{2\zeta_b}{\mu_1\phi_1^2} + \frac{1}{2\zeta_p}\right)^2} \quad (10)$$

Equation (9) shows that vibration response of SMD-structure model is a function of frequency ratio, α , mass ratio μ_1 , pedestrian and bridge damping ratios and mode shape of the bridge, ϕ_1 .

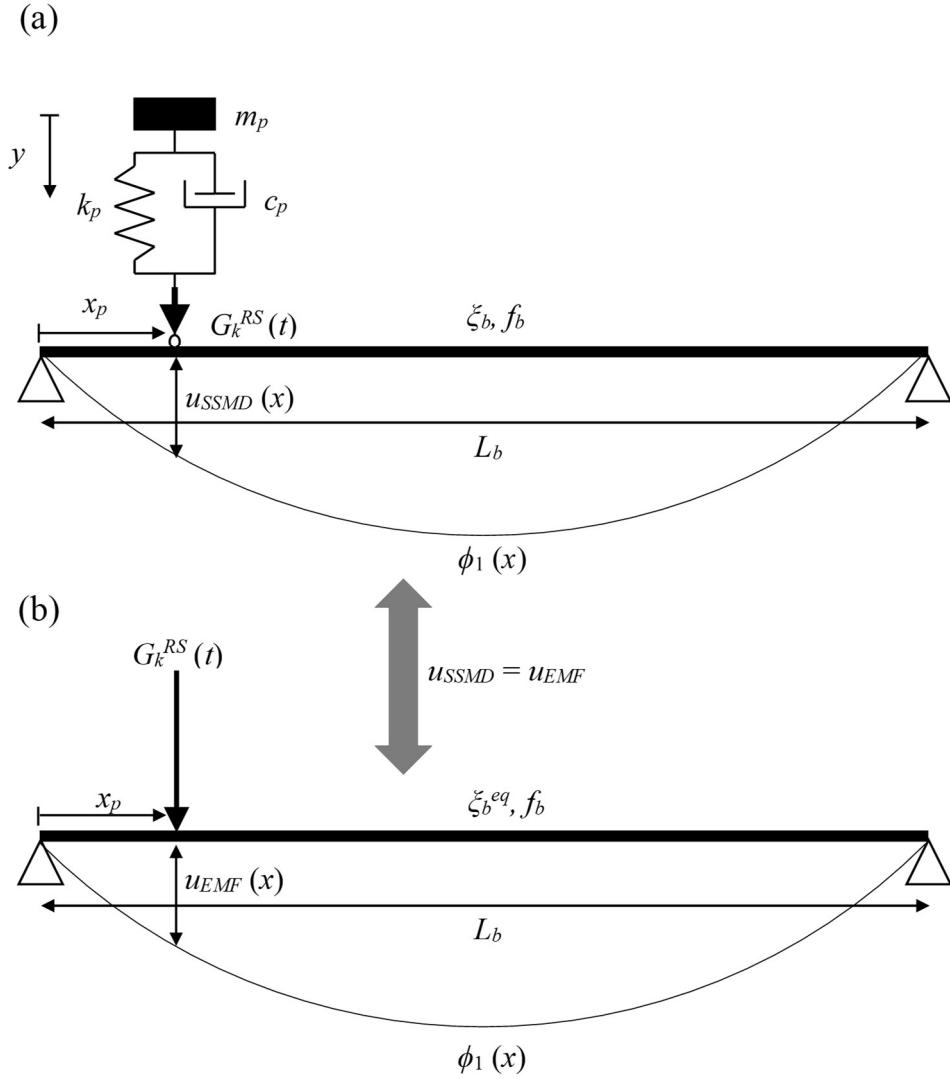


Figure 6. (a) Stationary (walking on the spot) spring-mass-damper model, and (b) equivalent moving force model.

3.4 Simulation example

Representation of the frequency and damping of structures plays a pivotal role in the accurate simulation of footbridge vibration response. For both footbridges, free decay vibration results show that the damping, ζ_b , and frequency, f_b , are amplitude-dependent. Thus, for numerical simulations, amplitude-dependent damping and frequencies are used in a cycle-by-cycle analysis to minimize the inaccuracies arising from poor representation of the footbridge properties ([42], [43]). Furthermore, the experimental modal analysis on both bridges showed that the relevant mode shapes can be described by half-sine function ([42], [43]), such that:

$$\phi_1(x) = \sin\left(\frac{\pi x}{L_b}\right) \quad (11)$$

Newmark- β integration was used to solve equations (3) and (7). Furthermore, the equivalent damping was determined at the mid-span ($\phi_1(x = L_b/2)$) using equation (9) and used in the EMF model for both footbridges.

For the three models described, Figure 7 shows the positive envelope of simulated vibration response of the MB for the exemplar test subject. To illustrate some features of different models, three sets of parameters are chosen to represent the test subject: $f_p = 1, 1.86,$ and 4.0 Hz and $\zeta_p = 0.05, 0.15,$ and $0.3,$ respectively, along with $m_p = 113$ kg. These are denoted MSMD1, MSMD2, and MSMD3, respectively, and the corresponding equivalent models are EMF1, EMF2, and EMF3. The MF model highly overestimates the vibration response for the exemplar test subject, compared to the measured vibration response (see Figure 3a). This shows the need for a more accurate model for structural vibration response predictions than the MF model currently used in guidelines. On the other hand, the MSMD model provides a range of responses which depend on the chosen parameters of the human. In particular, the parameters in MSMD2 result in a response that is relatively close to the measured response in terms of the peak vibration value. Interestingly, this occurs when the pedestrian natural frequency is close to the natural frequency of the bridge, and this point will be investigated in detail in Section 4.3. The simpler EMF models result in a close match to the corresponding MSMD model responses, as expected.

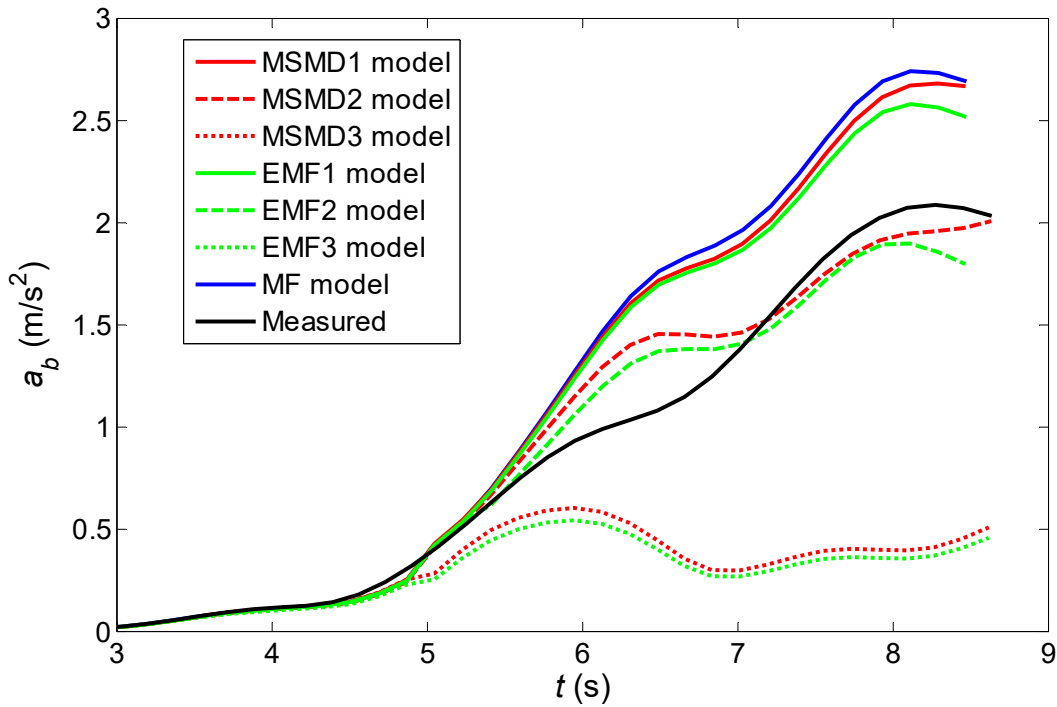


Figure 7. Positive Envelope of simulated vibration responses of the MF, and various MSMD and EMF models, shown with the measured vibration response for the exemplar test subject on the MB.

4. Calibration of MSMD Parameters

Calibration of the MSMD model is carried out to the vibration responses of the Monash Footbridge, as noted earlier. The best fit model parameters α , and ξ_p are determined. The mass of the MSMD model is taken as the mass of the pedestrian, m_p . The objective function is a least squares error between the model and measured responses.

4.1 Parametric study

Prior to application of an optimization routine to find the best fit parameters, a parametric study is conducted to find the feasible ranges of the MSMD model frequency ratio and damping. The considered bridge response metric is the maximum acceleration response, a_{max} . Alternatively, the 1s root mean square (RMS) trend could be used, but over a few cycles, these measures are proportional when the response is dominated by a single vibration mode, as is the case here [11], [49].

Figures 8a and 8b show the maximum acceleration response of the exemplar test subject versus MSMD-to-bridge frequency ratio ($\alpha = f_p/f_b$) for a wide range of the MSMD model damping ratios, ζ_p . At small α values, the MSMD response (especially for lower values of ζ_p) approaches the MF response. For both footbridges, an increase in α leads to a decrease in the vibration response for α up to about 1 (see Figures 8a and 8b). For $\alpha > 1$, the vibration response roughly increases with increasing α until it reaches a constant value. For the WB, this constant value is identical to the MF vibration response while for the MB, it is far lower than the MF response. Furthermore, at α values far enough from 1, an increase in ζ_p reduces the vibration response whereas at α values around 1, the effect of ζ_p becomes such that it increases the vibration response (see Figures 8a and 8b). For ζ_p values higher than 0.6, the change in MSMD model response is very small (Figures 8a and 8b) and so 0.6 is chosen as the maximum value for the MSMD model damping range of the investigation.

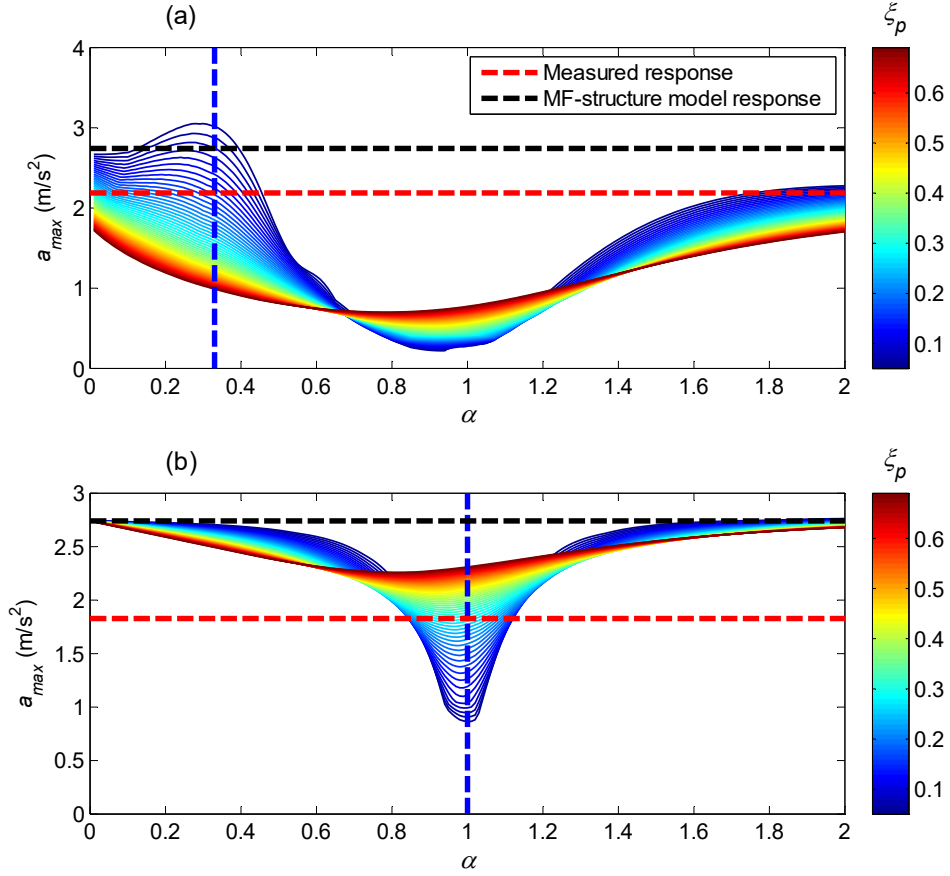


Figure 8. Effects of the MSMD model frequency and damping on vibration response of: (a) MB, and (b) WB for the exemplar tests and trials.

Interestingly, these results are hinted at by the simpler closed-form approach of the EMF model. As seen in equation (9), when α approaches zero, $1/\alpha$ approaches infinity. $1/\alpha^4$ approaches infinity faster than $1/\alpha^2$ and the ξ_b^{eq} limit is ξ_b , which means the response approaches the MF response (see Figures 8a and 8b). Equation (10) clearly shows that, at $\alpha=1$, equivalent MF damping reduces with increasing damping of SMD, leading to lower responses (Figure 8b). If α approaches infinity, i.e. relatively high values, equation (9) reduces to:

$$\xi_b^{eq} = \xi_b \sqrt{\left(\frac{\mu_1 \phi_1^2}{2\xi_b}\right)^2 + 1} \quad (12)$$

As the Warwick footbridge (WB) has a very low mass ratio, μ_1 , the term under square root in equation (12) is close to 1, and thus ξ_b^{eq} is very close to ξ_b resulting in a similar vibration

response to that of the MF model (Figure 8b). On the other hand, the high mass ratio of the MB leads to an equivalent damping far higher than the bridge damping, and hence a vibration response far lower than the MF response (Figure 8a).

The feasible ranges for the MSMD model parameters are identified as those resulting in intersection with the corresponding measured vibration responses in Figures 8a and 8b. For the MB, the MSMD models with α around the third harmonic of walking force, $\alpha \approx 0.33$, are good matches with the measured vibration response (Figure 8a). This might be the first mode of human body which interacts with the bridge. Note that $\alpha \approx 2$ also gives good matches with the measured vibration response which possibly indicates influence of second mode of human body on the response of MB. For the WB, MSMD models with α around the first harmonic of walking force, $\alpha \approx 1$, are good fits for the measured values (Figure 8b).

As different bridges give different feasible α parameter ranges, a new parameter is defined, $\beta = kf_p/f_b = k\alpha$, for the k th harmonic of walking force in resonance with the footbridge. For $\beta \approx 1$, MSMD models are viable for a good match between simulated and measured vibration responses for both footbridges as shown in Figure 9 for the Monash bridge. For the Monash bridge, the third harmonic of walking is in resonance with the bridge (i.e. $k = 3$, and thus $\beta = 3f_p/f_b = 3\alpha$). For the Warwick bridge, it is the same as Figure 8b as the first harmonic of walking force is in resonance with the bridge (i.e. $k = 1$, and thus $\beta = \alpha$). Expressed in this way, β includes the resonant harmonic number and generic MSMD model parameters, making it useable for footbridges with different frequencies. Therefore, the optimum MSMD model parameters will be found in two-dimensional parameter space of β and ζ_p , within estimated ranges of 0.5-1.5 and 0-0.6, respectively.

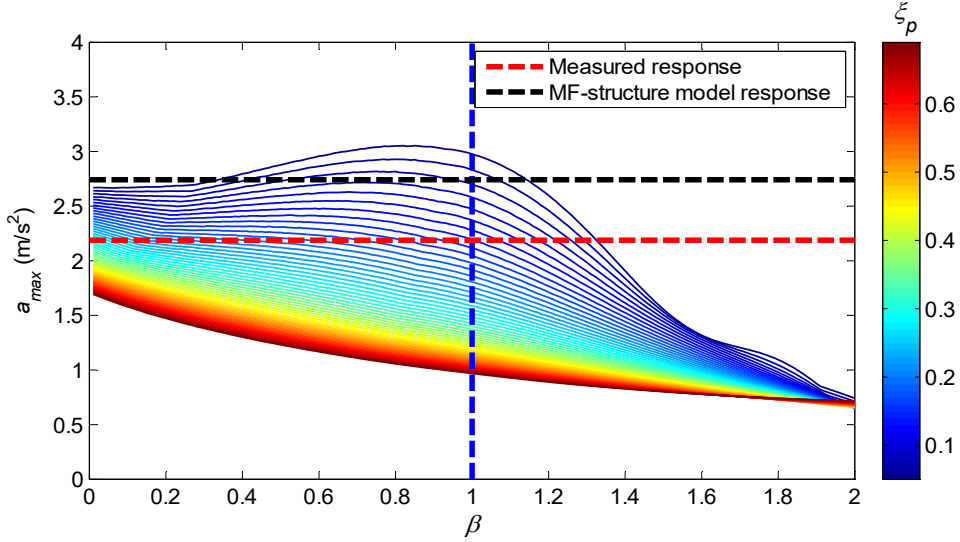


Figure 9. Effects of the MSMD model damping on vibration response versus β parameter for the MB ($k = 3$, third harmonic of walking considered).

4.2 Two-dimensional parameter space error

An optimal pair of frequency parameter and damping ratio for the MSMD model is sought over a two-dimensional parameter space, β and ξ_p to find the best match between the MSMD model response, R^{MSMD} , and the response measured in resonance trials, R^M . A test subject is indicated by the index, i , of which there are n ($n = 18$) and index j is used to denote a specific trial of which there are $N = 15$ for each test subject at resonant walking. Since the GRF on the rigid surface is measured N times, there are N MSMD model responses for each test subject at the resonant pacing frequency. There, to determine a relative error over the two-dimensional parameter space for the i th test subject, the following steps are employed:

1. Determine the mean of the measured responses across the N trials at the resonant pacing frequency:

$$\bar{R}_i^M = \frac{1}{N} \sum_{j=1}^N R_{ij}^M \quad (13)$$

2. For a specific parameter pairing, take the mean of MSMD model responses across the N trials due to the i th test subject ($i = 1, \dots, 18$):

$$\bar{R}_i^{MSMD}(\beta, \xi_p) = \frac{1}{N} \sum_{j=1}^N R_{ij}^{MSMD}(\beta, \xi_p) \quad (14)$$

3. Determine the relative error for these parameter values for i th test subject:

$$E_i(\beta, \xi_p) = \frac{\bar{R}_i^M - \bar{R}_i^{MSMD}(\beta, \xi_p)}{\bar{R}_i^M} \quad (15)$$

The sum of the squared relative errors between the mean measured and MSMD-structure model response metrics across all test subjects is used as the global objective function:

$$E(\beta, \xi_p) = \sum_i^n E_i^2(\beta, \xi_p) \quad (16)$$

In previous limited studies on the MSMD model parameters calibration, the objective function was to reduce the error between the measured and simulated acceleration responses at the waist of the pedestrian in the frequency domain ([50], [38]). However, for vibration serviceability assessment of structures, an estimation of vibration response of the structure is required for comparison with the acceptability criteria stipulated by design codes or guidelines. Hence, here the objective function (equation (16)) quantifies the error between the measured and MSMD model footbridge vibration responses.

4.3 Optimization

Figure 10a shows the relative error contours over the two-dimensional parameter space of β and ξ_p for the exemplar test subject. Contours follow a diagonal trend, which can be explained by reference to Figure 8a. Further, there is always a zero-error contour for a specific test subject, as shown by the red line in Figure 10a. Figure 10b shows the objective function (see equation (16)) over the parameter space of β and ξ_p for all test subjects. As seen, there is an area (see Figure 10b, the area enclosed by red line) within which the objective function value is minimal. To find the optimum pair of β and ξ_p inside this area, a quadratic surface was fitted points around this area, and the surface minimum value was found to be 1.197 at $\beta = 0.988$ and $\xi_p = 0.23$, shown by a black point in Figure 10b. For simplicity the optimum β is taken as $\beta_{op} = 1$ as the difference in the objective function between $\beta = 1$ and $\beta = 0.988$ for $\xi_p = 0.23$ is very

small (0.07%). This result suggests that, on average, pedestrians can be modelled as having $\beta_{op} = 1$, i.e. $f_p = f_b/k$ to account for HSI at resonance. $\beta_{op} = 1$ obtained here shows the resonance between MSMD and walking force (i.e. $f_p = f_w$) which is interestingly the assumption made by Zhang et al [41] for their proposed SMD model. Note that $f_p = f_w$ does not mean that the pedestrian frequency is always equal to walking frequency; however, it gives the best fit between simulated MSMD and measured vibration responses for all test subjects and resonant walking trials.

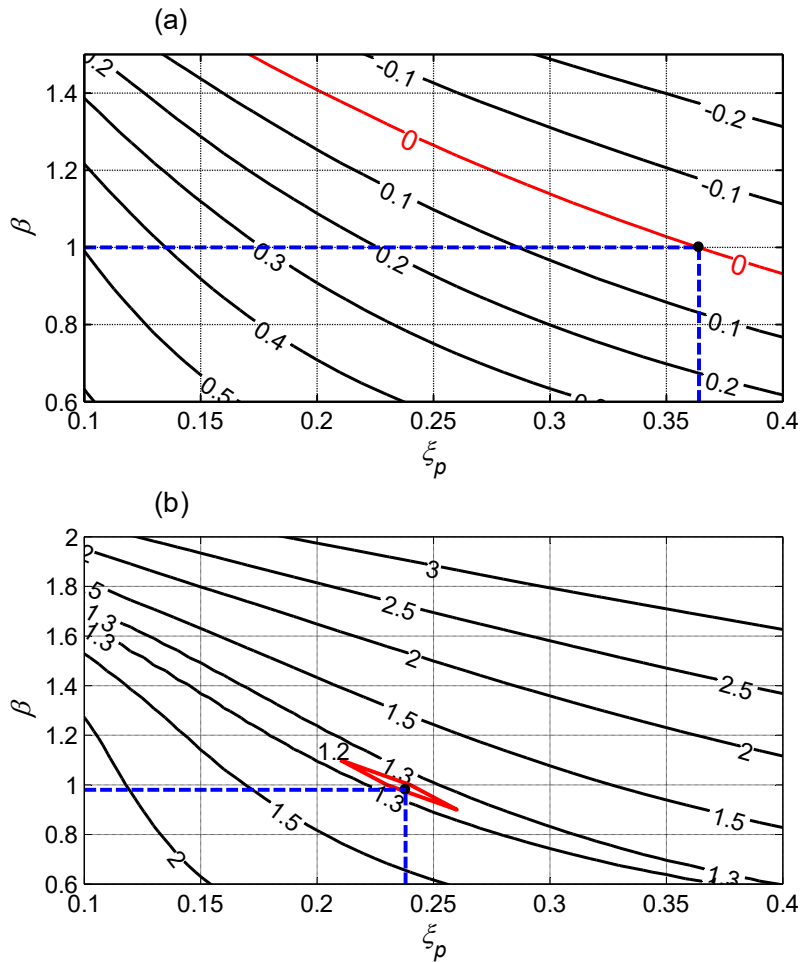


Figure 10. (a) Relative error contours for the exemplar test subject, and (b) objective function contours for all test subjects showing minimum over the two-dimensional parameter space.

The ξ_p obtained from the optimization is a global optimum damping for all test subjects. However, it is hypothesized that this parameter varies with test subject mass, since we imagine skeleton masses to be roughly similar and fat/muscle to contribute damping. Using $\beta_{op} = 1$, an

optimum damping for each test subject is determined. In Figure 10a, for the exemplar test subject, this optimum damping is seen to be $\xi_{op}^p = 0.36$. This procedure is used to obtain optimum damping values for all 18 test subjects. Figure 11 shows the optimal damping against test subject mass (in kg), along with an empirical curve fit, given by:

$$\xi_{op}^p = 0.38 \ln(m_p) - 1.42 \quad (17)$$

The optimal damping of the MSMD model increases with pedestrian mass, which acknowledges the higher effects of HSI for heavier test subjects. This result differs from the assumption of constant SMD damping ratio made by Zhang et al. [41], indicating that their model might not be suitable for a wide range of pedestrians. It should be noted that this proposed model ignores the change in the walking frequency due to the vibrating bridge surface [41].

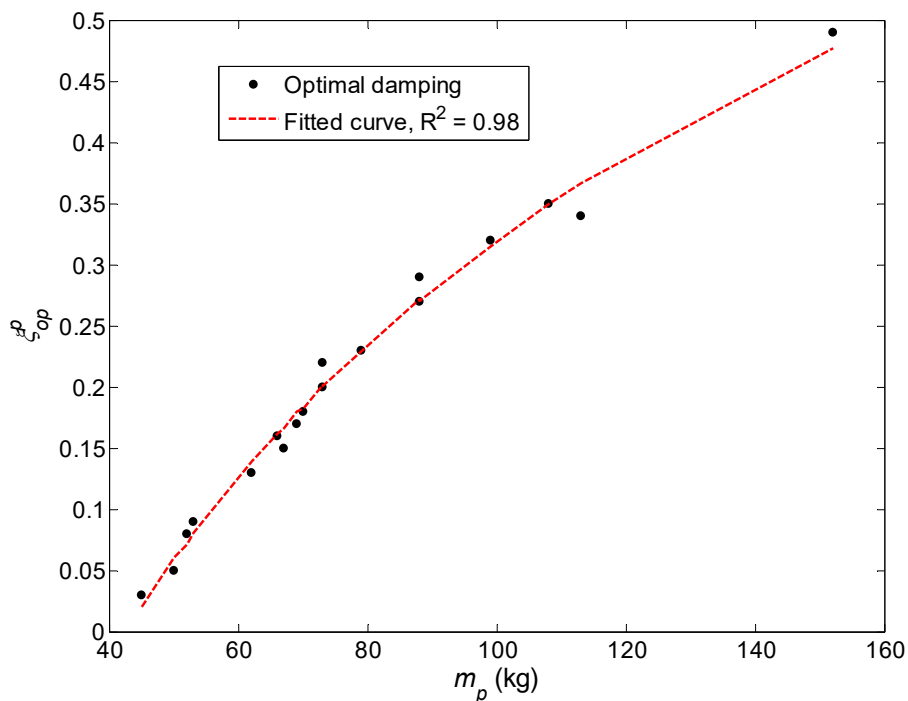


Figure 11. Optimal damping of the MSMD model for all test subjects.

5. Proposed Models

5.1 Optimal MSMD and EMF models

Figure 12 shows the overview of the calibrated models. The identified MSMD model parameters suggested in this study are: (1) m_{op}^p is the pedestrian mass; (2) f_{op}^p is the resonant walking frequency at harmonic k , f_b/k , ($f_{op}^p = f_b/k$) and; (3) ζ_{op}^p is determined using equation (17) using the pedestrian mass. These parameters can be used in an MSMD-structure model to determine footbridge vibration response (part (b)). It should be noted that since normal walking frequency, f_w , falls within 1.6-2.4 Hz [13], the critical harmonic k (integer) is selected such that $f_b \in [1.6k \ 2.4k]$, so that the footbridge is in resonance with the k th harmonic of walking force. For engineering practice, the simpler EMF can be used by determining the equivalent damping of the footbridge, ζ_b^{eq} , using equation (9) (part (c)) with the optimal MSMD inputs as identified, and using this bridge damping in a conventional moving force model to determine the vibration response of the footbridge (part (d)).

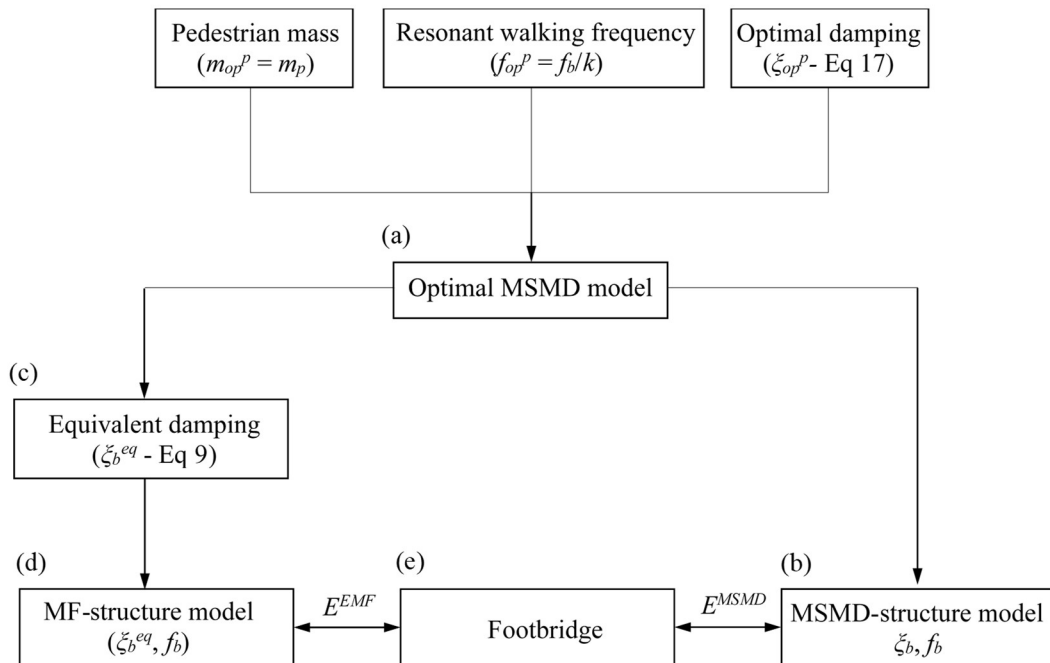


Figure 12. Overview of the proposed MSMD and EMF models for including human-structure interaction effects.

5.2 Model validation

To validate the results of the proposed MSMD and EMF models, the experimental results of the full-scale Warwick footbridge (WB), were used. As an example, Figure 13a shows positive envelope of the measured, MSMD model, and EMF model vibration response time histories of the WB for the exemplar test subject and trial. The proposed MSMD and EMF models give vibration responses which are close to the measured response. A shift in the maximum amplitude of the response, however, is seen due to the slight difference between calculated and real bridge frequency.

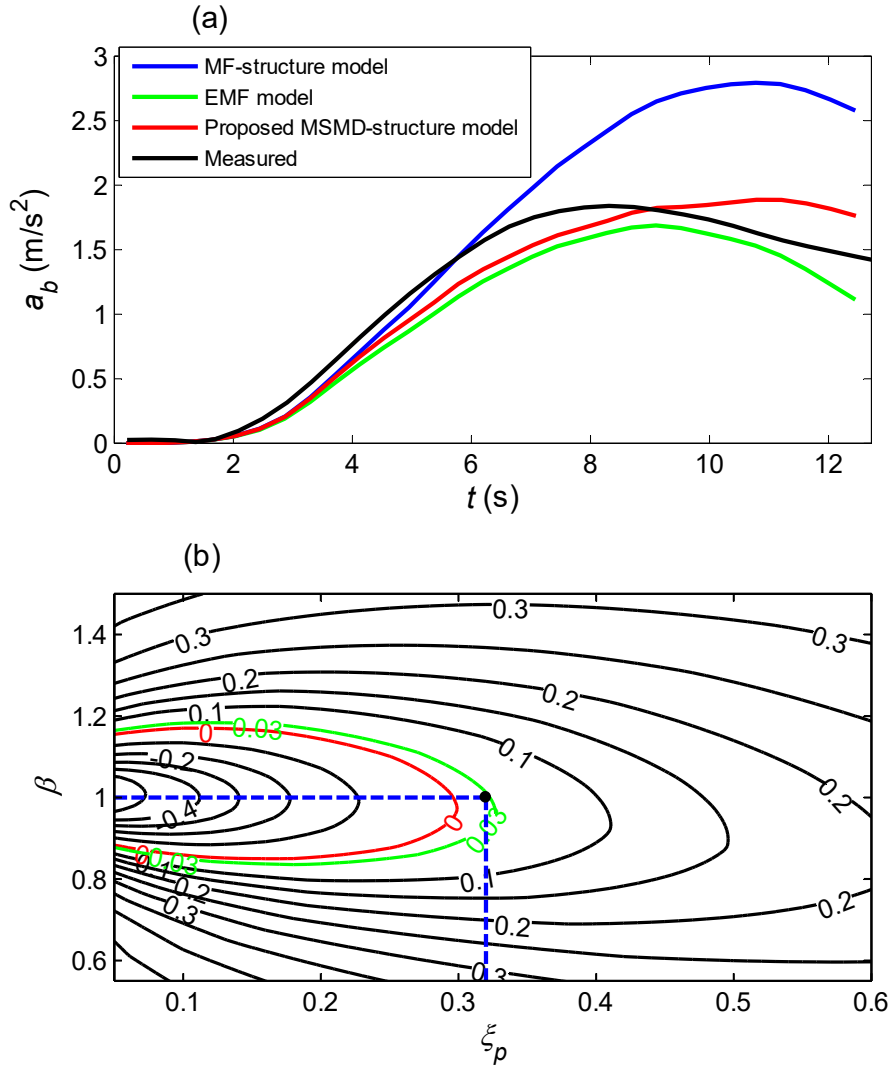


Figure 13. Exemplar test subject for Warwick footbridge: (a) positive envelope of acceleration time history; (b) the proposed MSMD model relative error contour.

The relative error contours are also constructed using procedure explained in section 4.2 for the exemplar test subject of the WB (Figure 13b). The red contour line shows the zero-error contour between the measured and MSMD model. The black point shows the parameters of the proposed MSMD model from the MB. Notably, this corresponds to a small error (0.03).

The mean relative errors over all walking trials including the MF model error, E^{MF} , proposed MSMD model error, E^{MSMD} , and EMF model error, E^{EMF} , for all test subjects of the WB are

determined (see Figure 12 for E^{EMF} and E^{MSMD}) and summarized in Table 4. The much smaller E^{MSMD} values compared to E^{MF} values indicate significant improvements in the vibration response prediction using the proposed MSMD model. The MSMD model accuracy becomes clearer for heavier test subjects, where human-structure interaction is more pronounced. In these cases a great error reduction is observed using the proposed MSMD model. Although the EMF is based on a continuous walking force model and an equivalent damping ratio at the bridge frequency [51], ignores walking frequency variations, and considers only stationary response of the bridge, the small relative errors for the EMF model indicate reliable performance of the EMF model in the vibration response estimation using optimal MSMD parameters.

Table 4. The MF, proposed MSMD, and EMF models mean relative error.

Test subject	μ (%)	ξ_{op}^p	E_i^{MF}	E_i^{MSMD}	E_i^{EMF}
1	0.73	0.10	-0.04	0.09	0.10
2	0.86	0.16	-0.07	0.11	-0.08
3	1.06	0.24	-0.42	-0.04	0.05
4	1.30	0.32	-0.64	0.03	0.08
5	1.49	0.37	-0.51	-0.07	0.10

6. Conclusion

In this study, an experimental-numerical approach is adopted to find an optimal moving spring-mass-damper model for human-structure interaction consideration. A large number (295) of walking trials are performed on two lively footbridges for a wide range (23) of test subjects, all with normal gait. A parametric analysis was conducted on MSMD parameters using results of both bridges. The experimental results of one footbridge were used for the MSMD model parameters optimization, and the second footbridge results used to test the validity of the proposed MSMD model. For the calibration purpose, the sum of the squared relative errors between the MSMD model and measured vibration responses for all test subjects was

minimized to find the optimal frequency for the MSMD model. The optimal frequency was then used for each test subject separately to determine optimal damping of the MSMD model.

The proposed MSMD model takes pedestrian actual mass as the mass parameter of the model. The model frequency is the resonant walking frequency, and an empirical relationship is suggested for the model damping as a function of pedestrian mass. The results of the model validation on a different bridge show a good agreement between the measured vibration response and the vibration response predicted by the model. Thus, the calibrated MSMD can be used to significantly improve the vibration response estimates compared to the standard moving force model.

Finally, this study argues that simpler version of the MSMD model—the equivalent moving force model—is a reliably accurate and simple means suitable for use in engineering practice. This method is easy to implement in engineering practice since it uses the well-known moving force model with a modified damping for the footbridge. The modelling approach proposed in this paper has potential to be used in updating the models currently available in the design recommendations. It is a rare example of successful calibration of the MSMD model for simulating pedestrian interaction effects with bridges excitable by different forcing harmonics. The authors invite other researchers to investigate applicability of the proposed model on a wider range of full-scale footbridges of different dynamic properties.

Acknowledgements

This work was funded by a Monash-Warwick Alliance Seed Grant and a Monash Graduate Scholarship (MGS).

References

- [1] S. Živanović, Benchmark Footbridge for Vibration Serviceability Assessment under the Vertical Component of Pedestrian Load, *J. Struct. Eng.* 138 (2012) 1193–1202. [https://doi.org/10.1061/\(ASCE\)ST.1943-541X.0000571](https://doi.org/10.1061/(ASCE)ST.1943-541X.0000571).
- [2] S. Živanović, A. Pavić, E.T. Ingólfsson, Modeling spatially unrestricted pedestrian traffic on footbridges, *J. Struct. Eng.* 136 (2010) 1296–1308. [https://doi.org/10.1061/\(ASCE\)ST.1943-541X.0000226](https://doi.org/10.1061/(ASCE)ST.1943-541X.0000226).
- [3] E. Shahabpoor, A. Pavic, V. Racic, Interaction between walking humans and structures in vertical direction: a literature review, *Shock Vib.* 2016 (2016) 12–17. <https://doi.org/10.1155/2016/3430285>.
- [4] P.J. Fanning, P. Archbold, A. Pavic, A Novel Interactive Pedestrian Load Model for Flexible Footbridges, in: *SEM Annu. Conf. Expo. Exp. Appl. Mech.*, 2005: pp. 1–8.
- [5] C.C. Caprani, E. Ahmadi, Formulation of human-structure system models for vertical vibration, *J. Sound Vib.* (2016). <https://doi.org/http://dx.doi.org/10.1016/j.jsv.2016.05.015>.
- [6] K. Van Nimmen, G. Lombaert, G. De Roeck, P. Van den Broeck, The impact of vertical human-structure interaction on the response of footbridges to pedestrian excitation, *J. Sound Vib.* 402 (2017) 104–121. <https://doi.org/10.1016/j.jsv.2017.05.017>.
- [7] OHBDC, Ontario Highway Bridge Design Code, Highway Engineering Division, Ministry of Transportation and Communication, Ontario, Canada, 1983.
- [8] BSI (British Standards Institution). U.K. national annex to Euro- code 1: Actions on structures—Part 2: Traffic loads on bridges. EN 1991-2:2003, London., 2008.
- [9] ISO 10137 - Bases for design of structures - Serviceability of buildings and walkways against vibrations, 1992.
- [10] Eurocode 5, Design of Timber Structures—Part 2: Bridges, ENV 1995-2: 1997, European Committee for Standardization, (1997).
- [11] Sétra, Guide méthodologique passerelles piétonnes (Technical guide Footbridges: assessment of vibrational behaviour of footbridges under pedestrian loading), 2006.
- [12] Design of footbridges – HIVOSS (Human Induced Vibrations of Steel Structures), 2009.
- [13] E. Ahmadi, C.C. Caprani, A. Heidarpour, An equivalent moving force model for consideration of human-structure interaction, *Appl. Math. Model.* 51 (2017) 526–545. <https://doi.org/10.1016/j.apm.2017.06.042>.
- [14] M. Willford, Dynamic actions and reactions of pedestrians, in: *Proc. Int. Conf. Des. Dyn. Behav. Footbridges*, Paris, France, 2002: pp. 66–73.
- [15] S. Živanović, I.M. Diaz, A. Pavić, Influence of walking and standing crowds on structural dynamic properties, in: *27th IMAC Conf.*, Orlando, USA, 2009.
- [16] M. Kasperski, Damping induced by pedestrians, in: *9th Int. Conf. Struct. Dyn. EURO DYN*, Porto, Portugal, 2014: pp. 1059–1064.

- [17] E. Bassoli, K. Van Nimmen, L. Vincenzi, P. Van den Broeck, A spectral load model for pedestrian excitation including vertical human-structure interaction, *Eng. Struct.* 156 (2018) 537–547. <https://doi.org/10.1016/j.engstruct.2017.11.050>.
- [18] S.V. Ohlsson, Floor vibrations and human discomfort, PhD Thesis, Göteborg, Sweden, Chalmers University of Technology, 1982.
- [19] K. Baumann, H. Bachmann, Durch menschen verursachte dynamische lasten und deren auswirkungen auf balkentragwerke, Swiss Federal Institute of Technology (ETH), Zürich, Switzerland, 1988.
- [20] R.L. Pimentel, Vibrational performance of pedestrian bridges due to human-induced loads, 1997.
- [21] H.V. Dang, S. Živanovic, Influence of low-frequency vertical vibration on walking locomotion, *J. Struct. Eng.* 142 (2016) 1–12. [https://doi.org/10.1061/\(ASCE\)ST.1943-541X.0001599](https://doi.org/10.1061/(ASCE)ST.1943-541X.0001599).
- [22] P. Young, Improved floor vibration prediction methodologies, ARUP vibration seminar, 2001.
- [23] S.C. Kerr, Human Induced Loading on Staircases, 1998. [https://doi.org/10.1016/S0141-0296\(00\)00020-1](https://doi.org/10.1016/S0141-0296(00)00020-1).
- [24] V. Racic, A. Pavic, J.M.W. Brownjohn, Experimental identification and analytical modelling of human walking forces: Literature review, *J. Sound Vib.* 326 (2009) 1–49. <https://doi.org/10.1016/j.jsv.2009.04.020>.
- [25] C.R. Lee, C.T. Farley, Determinants of the center of mass trajectory in human walking and running, *J. Exp. Biol.* 201 (1998) 2935–2944.
- [26] A. Arampatzis, G.P. Brüggemann, V. Metzler, The effect of speed on leg stiffness and joint kinetics in human running, *J. Biomech.* 32 (1999) 1349–53.
- [27] L. Zhang, D. Xu, M. Makhsous, F. Lin, Stiffness and viscous damping of the human leg, in: 24th Annu. Meet. Am. Soc. Biomech., Chicago, 2000.
- [28] S. Rapoport, Constant and Variable Stiffness and Damping of the Leg Joints in Human Hopping, *J. Biomech. Eng.* 125 (2003) 507. <https://doi.org/10.1115/1.1590358>.
- [29] G.A. Bertos, S.M. Ieee, D.S. Childress, M. Ieee, S. a Gard, The vertical mechanical impedance of the locomotor system during human walking with applications in rehabilitation, in: *Proc. 9th Int. Conf. Rehabil. Robot.*, 2005: pp. 380–383.
- [30] H. Geyer, A. Seyfarth, R. Blickhan, Compliant leg behaviour explains basic dynamics of walking and running, *Proceedings. Biol. Sci., The R. Soc.* 273 (2006) 2861–7. <https://doi.org/10.1098/rspb.2006.3637>.
- [31] M.K. Lebedowska, T.M. Wenthe, M. Dufour, The influence of foot position on body dynamics, *J. Biomech.* 42 (2009) 762–6. <https://doi.org/10.1016/j.jbiomech.2008.12.021>.
- [32] P. Archbold, Interactive Load Models for Pedestrian Footbridges, National University of Ireland, 2004.
- [33] C.C. Caprani, J. Keogh, P. Archbold, P. Fanning, Characteristic vertical response of a footbridge due to crowd loading, in: *Eurodyn 2011 - Eighth Eur. Conf. Struct. Dyn.*,

- Leuven, Belgium, 2011: pp. 978–985.
- [34] P. Archbold, J. Keogh, C.C. Caprani, P. Fanning, A Parametric Study of Pedestrian Vertical Force Models for Dynamic Analysis of Footbridges, in: *EVACES – Exp. Vib. Anal. Civ. Eng. Struct.*, 2011: pp. 35–44.
- [35] R. Hashim, T. Ji, P. Mandal, Q. Zhang, D. Zhou, Human-structure interaction experiments to determine the dynamic properties of the standing human body in vertical vibration, *Structures*. 26 (2020) 934–946. <https://doi.org/10.1016/j.istruc.2020.04.040>.
- [36] J. Xiong, J. Chen, C. Caprani, Spectral analysis of human-structure interaction during crowd jumping, *Appl. Math. Model.* 89 (2021) 610–626. <https://doi.org/10.1016/j.apm.2020.07.030>.
- [37] F.T. da Silva, R.L. Pimentel, Biodynamic walking model for vibration serviceability of footbridges in vertical direction, in: *8th Int. Conf. Struct. Dyn. EUROLYN*, 2011: pp. 1090–1096.
- [38] M.A. Toso, H.M. Gomes, F.T. da Silva, R.L. Pimentel, Experimentally fitted biodynamic models for pedestrian-structure interaction in walking situations, *Mech. Syst. Signal Process.* 72–73 (2015) 590–606. <https://doi.org/10.1016/j.ymsp.2015.10.029>.
- [39] M. Bocian, J.M.W. Brownjohn, V. Racic, D. Hester, A. Quattrone, L. Gilbert, R. Beasley, Time-dependent spectral analysis of interactions within groups of walking pedestrians and vertical structural motion using wavelets, *Mech. Syst. Signal Process.* 105 (2018) 502–523. <https://doi.org/10.1016/j.ymsp.2017.12.020>.
- [40] M. Zhang, C.T. Georgakis, W. Qu, J. Chen, SMD model parameters of pedestrians for vertical human-structure interaction, in: *IMAC XXXIII A Conf. Expo. Struct. Dyn.*, 2015.
- [41] M. Zhang, C.T. Georgakis, J. Chen, Biomechanically Excited SMD Model of a Walking Pedestrian, *J. Bridg. Eng.* (2016) C4016003. [https://doi.org/10.1061/\(ASCE\)BE.1943-5592.0000910](https://doi.org/10.1061/(ASCE)BE.1943-5592.0000910).
- [42] E. Ahmadi, C. Caprani, S. Živanović, N. Evans, A. Heidarpour, A framework for quantification of human-structure interaction in vertical direction, *J. Sound Vib.* 432 (2018). <https://doi.org/10.1016/j.jsv.2018.06.054>.
- [43] E. Ahmadi, C. Caprani, S. Živanović, A. Heidarpour, Vertical ground reaction forces on rigid and vibrating surfaces for vibration serviceability assessment of structures, *Eng. Struct.* 172 (2018). <https://doi.org/10.1016/j.engstruct.2018.06.059>.
- [44] A. Forner Cordero, H.J.F.M. Koopman, F.C.T. Van Der Helm, Use of pressure insoles to calculate the complete ground reaction forces, *J. Biomech.* 37 (2004) 1427–1432. <https://doi.org/10.1016/j.jbiomech.2003.12.016>.
- [45] D.T.P. Fong, Y.Y. Chan, Y. Hong, P.S.H. Yung, K.Y. Fung, K.M. Chan, Estimating the complete ground reaction forces with pressure insoles in walking, *J. Biomech.* 41 (2008) 2597–2601. <https://doi.org/10.1016/j.jbiomech.2008.05.007>.
- [46] J.H. Rainer, G. Pernica, D.E. Allen, Dynamic loading and response of footbridges, *Can. J. Civ. Eng.* 15 (1988) 66–71. <https://doi.org/10.1139/l88-007>.

- [47] S. Yao, J.R. Wright, A. Pavic, P. Reynolds, Forces generated when bouncing or jumping on a flexible structure, in: ISMA, Leuven, Belgium, 2002: pp. 563–572.
- [48] J.E. Wheeler, Prediction and Control of Pedestrian-Induced Vibration in Footbridges, ASCE J. Struct. Div. 108 (1982) 2045–2065.
- [49] C. Dong, S. Bas, F.N. Catbas, Investigation of vibration serviceability of a footbridge using computer vision-based methods, Eng. Struct. 224 (2020) 111224.
<https://doi.org/10.1016/j.engstruct.2020.111224>.
- [50] M.A. Toso, H.M. Gomes, F.T. Silva, R.L. Pimentel, A Biodynamic Model Fit for Vibration Serviceability in Footbridges Using Experimental Measurements in a Designed Force Platform for Vertical Load Gait Analysis, in: Icem15 15Th Int. Conf. Exp. Mech., 2013: pp. 23–33.
- [51] S. Krenk, Dynamic Response to Pedestrian Loads with Statistical Frequency Distribution, J. Eng. Mech. 138 (2012) 1275–1281.
[https://doi.org/10.1061/\(ASCE\)EM.1943-7889.0000425](https://doi.org/10.1061/(ASCE)EM.1943-7889.0000425).